

Notoginsenoside R1 Elicits Inhibitory Effects on Keloid Fibroblasts via Downregulation of Vascular Endothelial Growth Factor

Weiping Huang, Jin Chen, Tao Zhu

Department of Plastic Surgery, Taizhou Central Hospital (Taizhou University Hospital), Taizhou, Zhejiang Province, China

Submitted: 03-Aug-2021

Revised: 17-Nov-2021

Accepted: 27-Apr-2022

Published: 19-Sep-2022

ABSTRACT

Background: Keloid is a fibrotic disease characterized by hyperproliferative fibroblasts. Notoginsenoside R1 (NGR1) possesses inhibitory roles on cell proliferation. Thus, the research sought to assess the mechanism of action of NGR1 against keloid. **Materials and Methods:** Cell viability of normal and keloid fibroblasts pretreated with different NGR1 concentrations was determined by Cell Counting Kit-8 assay. Cell cycle, apoptosis rate, and tube length were detected using flow cytometry and tube formation assay. Vascular endothelial growth factor (VEGF) expression was measured by quantitative real-time polymerase chain reaction and western blot. To verify the reversal effect of VEGF on NGR1, KEL FIB cells were transfected with pcDNA3-VEGF plasmids following treatment with 40 μ M NGR1; subsequently, the above indicators were determined again. **Results:** NGR1 decreased cell viability, and 20, 30, and 40 μ M NGR1 concentrations were selected for the next investigation. After KEL FIB was treated with NGR1, the apoptosis rate was increased, cell cycle was arrested, and tube formation was suppressed in a dose-dependent manner. The expression of VEGF was also suppressed. In further experiments, cell cycle and tube formation were promoted and apoptosis rate was decreased in NGR1-treated cells when VEGF was overexpressed. **Conclusion:** NGR1 may play as an inhibitor of endogenous VEGF, and NGR1 exerts its inhibitory effects on keloid fibroblasts by downregulating VEGF.

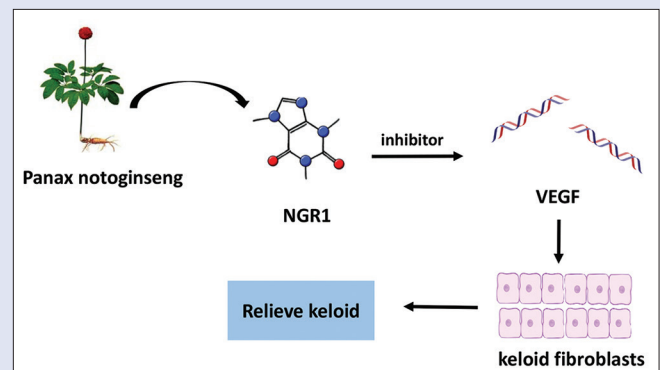
Key words: Apoptosis, cell cycle, keloid, notoginsenoside R1, vascular endothelial growth factor

SUMMARY

- In conclusion, our work provided evidence that NGR1 could act as an inhibitor of endogenous VEGF and exert inhibitory effects on keloid fibroblasts. Moreover, our findings showed that the natural product NGR1 may function as a candidate treatment drug for keloid prevention.

Abbreviations used: NGR1 = notoginsenoside R1, CCK-8 = Cell Counting Kit-8, qRT-PCR = quantitative real-time polymerase chain reaction, ECM = extracellular matrix, KFBs = keloid fibroblasts,

CASE = compounds like *Astragalus* and *Salvia miltiorrhiza* extract, CAG = chronic atrophic gastritis, TGF- β = transforming growth factor beta, VEGF = vascular endothelial growth factor, DMSO = dimethyl sulfoxide, PMSF = phenylmethanesulfonyl fluoride, SDS-PAGE = sodium dodecyl sulfate polyacrylamide gel electrophoresis, PVDF = polyvinylidene fluoride, CDS = coding sequence, SD = standard deviation. MSC = mesenchymal stem cells.



Correspondence:

Dr. Tao Zhu,
Department of Plastic Surgery, Taizhou Central Hospital (Taizhou University Hospital), 999 Donghai Avenue, Jiaojiang District, Taizhou, Zhejiang Province - 318 000, China.
E-mail: zhutao_zztiao@163.com
DOI: 10.4103/pm.pm_359_21

Access this article online

Website: www.phcog.com

Quick Response Code:



INTRODUCTION

Keloid, tumor-like fibrotic disease, represents an aberrant response to wound healing.^[1] Keloids are formed by proliferation, hemostasis, and inflammation processes, in which various growth factors and cytokines are involved.^[2] Keloid is characterized by hyperproliferative fibroblasts, hyperplastic capillaries and collagen, overdeposited extracellular matrix (ECM), as well as overgrown scars.^[3] The proliferation and apoptosis inhibition of keloid fibroblasts (KFBs) are the biological bases of scar formation.^[4] Scar therapies have always been difficult and hot topics in plastic surgery.^[5] Current therapies for scars, mainly including local corticosteroid, stress, cryotherapy, laser, and surgical therapy, are not uniformly successful.^[6] Therefore, novel alternative treatments are urgently needed. Importantly, several traditional Chinese medicines have been reported that exert soothing effects on scar, for example, compounds like *Astragalus* and *Salvia miltiorrhiza* extract (CASE), Tanshinone IIA, and Shikonin.^[7-9]

How ever, the biological action of notoginsenoside R1 (NGR1) in treating scar has not been observed.

NGR1, the main active components extracted from *Panax notoginseng*, possesses mitigating roles on atherosclerotic lesions, chronic atrophic gastritis (CAG), and cerebral ischemia-reperfusion injury,^[10-12] as well as possesses anti-inflammatory and antioxidative benefits.^[13,14] NGR1 has

This is an open access journal, and articles are distributed under the terms of the Creative Commons Attribution-NonCommercial-ShareAlike 4.0 License, which allows others to remix, tweak, and build upon the work non-commercially, as long as appropriate credit is given and the new creations are licensed under the identical terms.

For reprints contact: WKHLRPMedknow_reprints@wolterskluwer.com

Cite this article as: Huang W, Chen J, Zhu T. Notoginsenoside R1 elicits inhibitory effects on keloid fibroblasts via downregulation of vascular endothelial growth factor. Phcog Mag 2022;18:579-86.

been demonstrated to suppress vascular smooth muscle cell migration and proliferation.^[15] Zhu *et al.*^[16] also showed a clear correlation between NGR1 and apoptosis, inflammation, as well as oxidative stress. NGR1 has outstanding anti-inflammatory activity *in vitro* and *in vivo*.^[13,17-19] In addition, it has also been reported that keloid and hypertrophic scars are the result of chronic inflammation in reticular dermis.^[4] Thus, the present study sought to assess the beneficial effects and underlying mechanism of NGR1 against keloid.

Among the various biochemical factors involved in keloid formation, studies have mainly concentrated on growth factors such as transforming growth factor beta (TGF- β) and vascular endothelial growth factor (VEGF).^[20,21] VEGF, a positive angiogenic cytokine, has been confirmed to play a crucial role in wound healing.^[22] *In vitro* studies have demonstrated that overexpression of VEGF occurs during scar formation.^[23,24] Wu *et al.*^[21] indicated that dexamethasone-induced keloid regression occurs via downregulation of VEGF expression. In addition, NGR1 treatment could also markedly inhibit the level of VEGF, and thereby ameliorate diabetic retinopathy.^[25] These studies prove that VEGF likely exerts a crucial role in keloid formation, and NGR1 has a certain regulatory effect on VEGF. Therefore, we speculated that NGR1 can attenuate keloid through effective inhibition of VEGF expression.

In this study, to verify the above hypothesis, cell cycle, apoptosis rate, and tube formation were measured and the expression of VEGF was further determined after KFB was treated with NGR1. In addition, VEGF overexpression plasmid was synthesized to observe whether this operation can reverse the effect of NGR1. This study aims to investigate whether NGR1 could protect against keloid injury and what its regulatory mechanism is.

MATERIALS AND METHODS

Cell culture and treatment

Normal fibroblasts HDFa (PCS-201-012), HDFn (PCS-201-010), and KFB KEL FIB (CRL-1762) were obtained from ATCC (USA). KFB HKF (BFN6021621) was purchased from Qingqi Biotechnology Co., Ltd. (Shanghai, China), maintained in Dulbecco's modified Eagle's medium (DMEM; SH30243.01; Hyclone, Logan, UT, USA) supplemented with 10% fetal bovine serum (FBS; 10100147; Gibco, Grand Island, NY, USA) and penicillin-streptomycin solution (C0222; Shanghai, Beyotime, China), and stored in an incubator (370, Forma Steri-Cycle; Thermo Fisher, Waltham, MA, USA) at 37°C with 5% CO₂. Cells at passages 3–8 were used in the following experiments.

NGR1 was purchased from Solarbio Corporation (SN8230; Beijing, China) and dissolved in dimethyl sulfoxide (DMSO; D2650; Sigma-Aldrich, St. Louis, MO, USA). Normal fibroblast and KFB cells were treated separately with 0, 10, 20, 30, 40, 50 μ M NGR1 for 48 h in serum-free media to select the appropriate concentration.^[26] Subsequently, experiments were divided into four groups: control group (KEL FIB-untreated cells), low NGR1 group (KEL FIB cells were pretreated with 20 μ M NGR1), medium NGR1 group (KEL FIB cells were pretreated with 30 μ M NGR1), and high NGR1 group (KEL FIB cells were pretreated with 40 μ M NGR1).

Cell viability assay

The number of living keloid and normal fibroblasts was evaluated using a Cell Counting Kit-8 (CCK-8) assay following the instructions (CK04; Dojindo Molecular Technology, Kumamoto, Japan). Cells at exponential stage were plated in 96-well plates (3799; Corning Inc., Corning, NY, USA) with a density of 2×10^3 cells per well and then pretreated with different NGR1 concentrations for 48 h. Subsequently, 10 μ L

of CCK-8 reagent was added to the samples and cultured for another 1–4 h. The absorbance of each well was determined using a microplate reader (Multiskan SkyHigh, Thermo Fisher) at 450 nm, and cell viability was calculated.

Determination of cell cycle

KEL FIB cells were plated in six-well plates (3516, Corning Inc.) at a density of 3×10^5 cells/mL and then treated with three concentrations of NGR1. Subsequently, the samples were digested, harvested, suspended in phosphate-buffered saline (PBS; C0221A; Beyotime, Shanghai, China), and fixed at 4°C for 4 h with 70% ethanol. After washing twice, the cells were incubated with 500 μ L of propidium iodide (PI, 50 μ g/mL; P4170; Sigma, St. Louis, MO, USA) and 100 μ L of ribonuclease A (RNase A, 100 μ g/mL; R1030; Solarbio Corporation) at 4°C for 1 h. Cell cycle was detected by flow cytometry. For analyses, 10,000 cells were counted using Cell Quest software (BD Biosciences, San Jose, CA, USA), and the DNA data obtained were analyzed by ModFit software (Verity Software House, Topsham, ME, USA).

Apoptosis rate detection

Apoptosis rate in different groups was detected using Annexin V-fluorescein isothiocyanate (FITC)/PI staining (AD10-2; Dojindo Molecular Technology). Cells in six-well plates were harvested and washed using PBS after NGR1 treatment for 48 h, followed by suspension with binding buffer to determine the cell density of 1×10^6 /mL. Then 5 μ L FITC-Annexin V supplemented with 5 μ L PI was added to 100 μ L of the cell suspension for 15 min of staining in dark at room temperature. After that, the working solution was discarded and the results were expressed and analyzed using flow cytometer (FACSCalibur, BD Biosciences) and FlowJo software (FlowJo, LLC, Ashland, OR, USA).

Tube formation assay

Tube formation assay was conducted according to a previous study.^[27] Matrigel (354234; BD Biocoat, Bedford, MA, USA) was thawed overnight at 4°C in a refrigerator and added to a 96-well plate (3799, Corning Inc.) to gel at 37°C the next day. Then, the cells (2×10^4 cells/well) were plated on polymerized Matrigel and subsequently treated with NGR1 at 37°C for 6 h, as in the grouping described above. The tube structures were observed under an inverted microscope ($\times 100$, IX83; Olympus, Tokyo, Japan), and the total tube quantity was measured with ImageJ software (NIH Image, Bethesda, MD, USA).

Quantitative real-time polymerase chain reaction

Total RNA from NGR1-treated KEL FIB cells was isolated using a total RNA extraction kit (9767; Takara, Tokyo, Japan) according to the instructions. Spectrophotometry (NanoDrop, Thermo Fisher) and 1% agarose gel electrophoresis were used to determine the RNA concentration (ng/ μ L) and integrity, respectively. First-strand cDNA was then obtained using cDNA synthesis kit (6110A, Takara). Quantitative real-time polymerase chain reaction (qRT-PCR) was carried out in triplicate using SYBR mixture (DRR041B, Takara), cDNA templates, and forward–reverse primer in an Applied Biosystems[™] 7500 PCR instrument (ABI, Foster City, CA, USA) with glyceraldehyde-3-phosphate dehydrogenase (GAPDH) as the reference. Forty cycles (95°C for 10 s, 60°C for 30 s, and 72°C for 32 s) were conducted for amplification. 2^{− $\Delta\Delta$ C_t} method was used to analyze the relative expression.^[28] The primer sequences were as follows: VEGF (forward, 5'-CCCACTGAGGAGTCCAACAT-3'; reverse, 5'-TTATACCGGGATTCTTTCGCG-3'); GAPDH (forward, 5'-ATCCCATCACCATCTTCC-3'; reverse, 5'-GAGTCCTTCCACG ATACCA-3').

Western blot analysis

Cells with various treatments were harvested and lysed in RIPA buffer (R0010, Solarbio Corporation) containing 1% phenylmethanesulfonyl fluoride (PMSF; ST505; Beyotime, Shanghai, China) to extract total proteins, the concentration of which in each group was then detected with a BCA Protein Assay Kit (CW0014S; CWBIO, Beijing, China, <https://www.cwbio.com/search/index?keyword=CW0014S>). Equivalent quality of proteins (30 μ g) was separated by sodium dodecyl sulfate polyacrylamide gel electrophoresis (SDS-PAGE) and then transferred onto polyvinylidene fluoride membrane (PVDF; YA1701, Solarbio Corporation). Next, the membranes were blocked in 5% bovine serum albumin (BSA; SW3015, Solarbio Corporation) at room temperature for 1 h, which was subsequently followed by incubation with primary antibodies, anti-VEGF (ab32152, 151 kDa, 1/2000 dilution; Abcam, Cambridge, UK) and anti-GAPDH (ab226408, 36 kDa, 1/1000 dilution, Abcam), diluted with Tris-buffered saline and Tween 20 (TBST; T1085; Solarbio Corporation) overnight at 4°C. The next day, PVDF membranes were incubated with the corresponding Horse Radish Peroxidase (HRP)-conjugated secondary antibody (ab6721, 1/2000 dilution, Abcam; ab6728, 1/2000 dilution, Abcam) for 1 h. After washing for a total of 30 min, the protein bands were visualized using a chemiluminescence reagent (34577, Thermo Fisher) and Tanon chemical imaging system (Tanon-5200 Multi, Shanghai, China). ImageJ software was finally used to measure the relative protein expression.

VEGF overexpression experiment

PCR products of VEGF coding sequence (CDS) and pcDNA3.1 plasmid (VT1001, YouBao, Shanghai, China) after *Bam*HI and *Xho*I (81295-09-2 and 81295-43-4; Dalian Takara Biotechnology, Dalian, China) double enzyme digestion were ligated, transformed, and cloned to obtain pcDNA3-VEGF positive plasmids, which were then delivered to Shanghai Sangon Biotech for sequencing and identification. KEL FIB

cells were divided into three groups: NGR1 (KEL FIB cells only treated with 40 μ M NGR1), NGR1 + negative control (NC; KEL FIB cells treated with 40 μ M NGR1 and transfected with pcDNA3.1 plasmid), and NGR1 + VEGF (KEL FIB cells treated with 40 μ M NGR1 and transfected with pcDNA3-VEGF positive plasmid).

Cells were seeded in six-well plates 1 day in advance until they reached 80% confluency. Lipofectamine 3000 transfection reagent (L3000008; Invitrogen, Carlsbad, CA, USA) was then used to transfect the plasmid into cells in the grouping scheme as described above. According to the transfection protocol, for each well, 125 μ L of serum-free DMEM medium (SH30243.01, Hyclone) was used to dilute Lipofectamine and plasmid with incubation for 5 min, and subsequently, the above two diluted solutions was mixed and incubation for 5 min and the Lipofectamine-plasmid complex was added to each well. After culturing in an incubator at 37°C for 24 h, KEL FIB cells were collected for the determination of overexpression efficiency via qRT-PCR and western blot and for the subsequent evaluation of cell cycle, apoptosis rate, and tube formation.

Statistical analysis

Statistical analysis was performed using GraphPad 8.0 software (GraphPad, San Diego, CA, USA). The experiment was repeated three times. Data are expressed as means \pm standard deviation (SD). One-way analysis of variance (ANOVA) with Tukey's test was used for inter-group comparison. Significance was considered when the *P* values were <0.05 .

RESULTS

NGR1 pretreatment inhibited cell viability in normal fibroblasts and KFBs

To investigate the effect of NGR1 on cell viability and find an optimal concentration, normal fibroblasts (HDFa, HDFn) and KFB (HKF, KEL

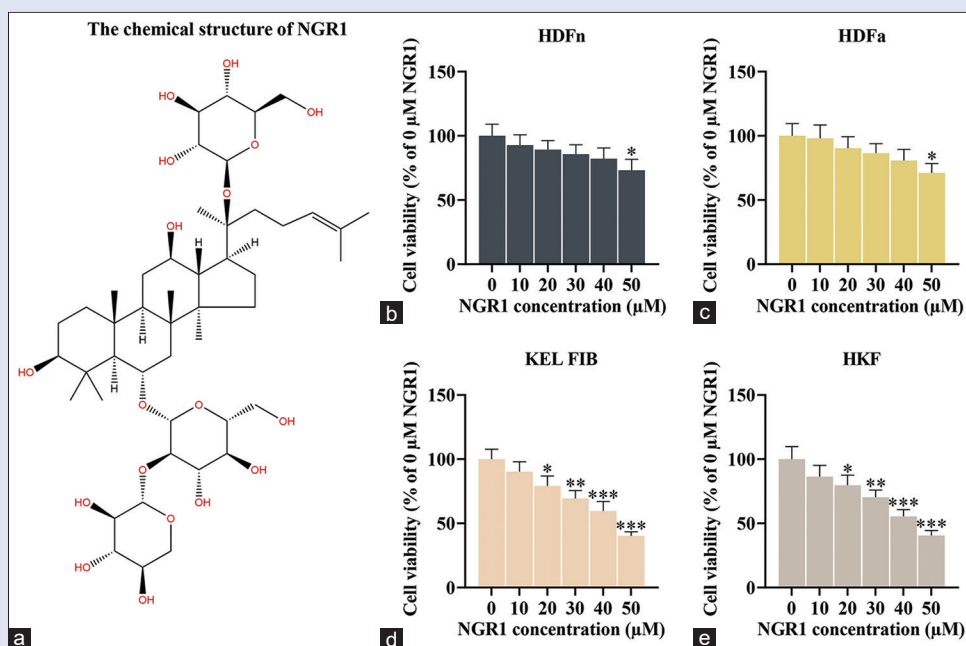


Figure 1: NGR1 treatment exerted an inhibitory effect on cell viability of normal fibroblasts (HDFa, HDFn) and keloid fibroblasts (HKF, KEL FIB). (a) Chemical structure of NGR1. (b–e) Cells were treated separately with 0, 10, 20, 30, 40, and 50 μ M NGR1 concentrations, and cells without NGR1 treatment were regarded as the control group. After incubation for 48 h, cell viability was evaluated using a CCK-8 assay. (b) Cell viability of HDFn cells. **P* < 0.05 versus 0 group. (c) Cell viability of HDFa cells. **P* < 0.05 versus 0 group. (d) Cell viability of KEL FIB cells. **P* < 0.05, ***P* < 0.01, ****P* < 0.001 versus 0 group. (e) Cell viability of HKF cells. **P* < 0.05, ***P* < 0.01, ****P* < 0.001 versus 0 group. Data are expressed as means \pm SD, and experiments were performed in triplicate CCK-8 = Cell Counting Kit-8, NGR1 = notoginsenoside R1, SD = standard deviation

FIB) were chosen and 0, 10, 20, 30, 40, and 50 μM NGR1 concentrations were designed for cell growth assessment by CCK-8 assay. Figure 1a shows the chemical structure of NGR1, whose molecular weight is 933 and molecular formula is $\text{C}_{47}\text{H}_{80}\text{O}_{18}$. As to the HDFa and HDFn cells, the cell viability was significantly reduced at 50 μM compared with untreated cells ($P < 0.05$) [Figure 1b and c]. Whereas for HKF, KEL FIB cells, a statistical difference in cell growth first appeared at 20 μM ($P < 0.05$) [Figure 1d and e]. Taken together, NGR1 concentrations of 20, 30, and 40 μM were selected for further experiments.

The effect of NGR1 treatment on KEL FIB cells

To verify the inhibition effect of NGR1 on KFB, we chose KEL FIB cells and tested the cell cycle, apoptosis rate, as well as tube formation. Results showed that NGR1 markedly induced G1 arrest at 20 μM , and with increased concentration, the inhibition effect was more obvious ($P < 0.05$) [Figure 2a and b]. Moreover, after 48 h of NGR1 treatment, the apoptosis rate showed an upward trend ($P < 0.05$) [Figure 2c and d] and the relative tube length was substantially suppressed ($P < 0.01$) [Figure 2e and f] in a dose-dependent manner compared with the control treatment. To further explore the inhibition mechanism of NGR1, the expression of angiogenic cytokine VEGF was determined by qRT-PCR and western blot. As shown in Figure 2g and h, statistical differences were observed between the experiment groups in VEGF mRNA and protein expressions after NGR1 treatment ($P < 0.01$). These results indicated that NGR1 is a suppressor of endogenous VEGF.

VEGF overexpression exerted a reversal effect on KEL FIB cells pretreated with NGR1

To verify the effectiveness of pcDNA3-VEGF plasmid, we first examined the expression of VEGF mRNA and Protein by qRT-PCR and western blot in KEL FIB cells pretreated with 40 μM NGR1 and transfected with the above overexpression plasmid (NGR1 + VEGF group). Results showed that VEGF mRNA and protein were remarkably increased in NGR1 + VEGF group when compared with NGR1 + NC group ($P < 0.001$) [Figure 3a and b]. After overexpression, the experiment can be successfully carried out; cell cycle was then detected by flow cytometry. As shown in Figure 3c and d, NGR1 and NGR1 + NC groups showed no obvious difference, VEGF overexpression reversed the arrest of cell cycle caused by NGR1 ($P < 0.001$).

VEGF overexpression suppressed cell apoptosis and induced tube formation

To further investigate the functional contributions of NGR1, a reversed verification experiment was carried out. KEL FIB cells were transfected with the pcDNA3-VEGF plasmid; apoptosis rate and tube formation were then detected. Data were visualized in the form of histogram and showed that [Figure 4a and b] the cell apoptosis rate of NGR1 + VEGF group dramatically decreased compared with NGR1 + NC group ($P < 0.01$). Furthermore, the tube length was markedly increased in NGR1+VEGF group compared with NGR1+NC groups ($P < 0.001$) [Figure 4c and d]. This analytical finding suggested that the effect observed in KEL FIB cells following NGR1 treatment was reversed by upregulating VEGF expression.

DISCUSSION

The current therapies used for keloids, such as local corticosteroid and cryotherapy, could induce adverse effects.^[6] Therefore, a safe, but also effective treatment should be put on the agenda. According to previous reports, traditional Chinese medicine and natural

products characterized by diverse pharmacological properties may be a potential therapeutic approach for keloid prevention; for example, Wubeizi ointment has been shown as an effective treatment for keloids^[29,30] and resveratrol could inhibit the proliferation and promote apoptosis of KFBs by targeting hypoxia inducible factor-1 α (HIF-1 α).^[31] Kawarazaki *et al.*^[32] found that sulfuraphane exerted inhibitory effect on collagen and cell growth in KFBs, indicating that it could be a novel treatment of keloid. NGR1, another kind of natural compounds, possesses high anti-inflammatory and antioxidative benefits. NGR1 has been used as a main bioactive compound in many traditional Chinese medicines clinically, such as Xuesaitong, Naodesheng, XueShuanTong, ShenMai, and QiShenYiQi.^[33-35] It has been demonstrated to be a potential therapy for prevention of various diseases such as diabetic retinopathy, CAG, and breast cancer.^[11,25,36] In this study, we explored the biological function of NGR1 and its potential mechanism in treating keloid injury.

Angiogenesis is a physiological phenomenon that has an important role in the formation of new blood vessels and endothelial cell proliferation, which can be regarded as an indicator to assess the impact of natural medicines on cell growth.^[37] NGR1 activates the Ang2/Tie2 pathway to promote angiogenesis.^[38] Apoptosis, a programmed cell death, plays vital roles in therapy of diverse diseases.^[39] A recent study has reported that luteolin may be a natural drug for keloid treatment by promoting apoptosis and regulating *FRAT1* gene expression.^[40] In this study, we found that NGR1 markedly suppressed cell viability and angiogenesis in a dose-dependent manner, markedly induced G1 stage arrest, and promoted cell apoptosis in KEL FIB cells. Whether it is NGR1 or luteolin, they inhibit keloid formation by promoting apoptosis, but the mechanisms involved may be different. Besides, cell cycle determines the cell fate to a large extent.^[41] For example, in an article about X-ray treatment of keloid, induction of cell senescence and suppression of proliferation were mediated by cell cycle interruption. Although the two therapeutic approaches of NGR1 and X-ray were not the same, the cell fates they brought about were very similar.^[42] Previous studies have reported that NGR1 treatment was effective in the migration, proliferation, cell cycle, and angiogenesis inhibition and apoptosis stimulation of MCF-7 cells.^[36] This is similar to our findings. Taken together, these results indicate that NGR1 has an inhibitory role on KFBs, not only by the way of inhibiting cell proliferation but also by promoting apoptosis, to protect patients from keloid injury.

While the beneficial effects of NGR1 against keloids have been investigated and various biological processes are found to be involved, the molecular mechanism still lacks clarity. Previous studies have elucidated that the molecular targets such as TGF- β and interleukin (IL)-6 could explain keloid pathogenesis.^[43,44] In addition, Stat3 has been demonstrated to contribute to keloid formation.^[45] Besides, Wu *et al.*^[21] showed regulation of VEGF may comprise a valuable effect on improving keloid. However, whether such molecular targets are involved in the inhibitory mechanism of NGR1 for keloid therapy has not been clarified. As an angiogenic cytokine, VEGF contributes to wound healing.^[23] Moreover, it has been proved that NGR1 treatment significantly decreased VEGF expression in diabetic retinopathy (DR).^[25] In the present study, NGR1 significantly inhibited the expressions of VEGF mRNA and protein of KEL FIB cells and the inhibition show concentration dependent. The same inhibitory relationship has been demonstrated in DR disease, as discussed above.^[25] The result shows that there exists a connection between NGR1 and VEGF; in other words, VEGF may be a treatment target for NGR1 in keloid. Here, we found that VEGF promoted cell cycle and tube formation and suppressed apoptosis of KFB, which

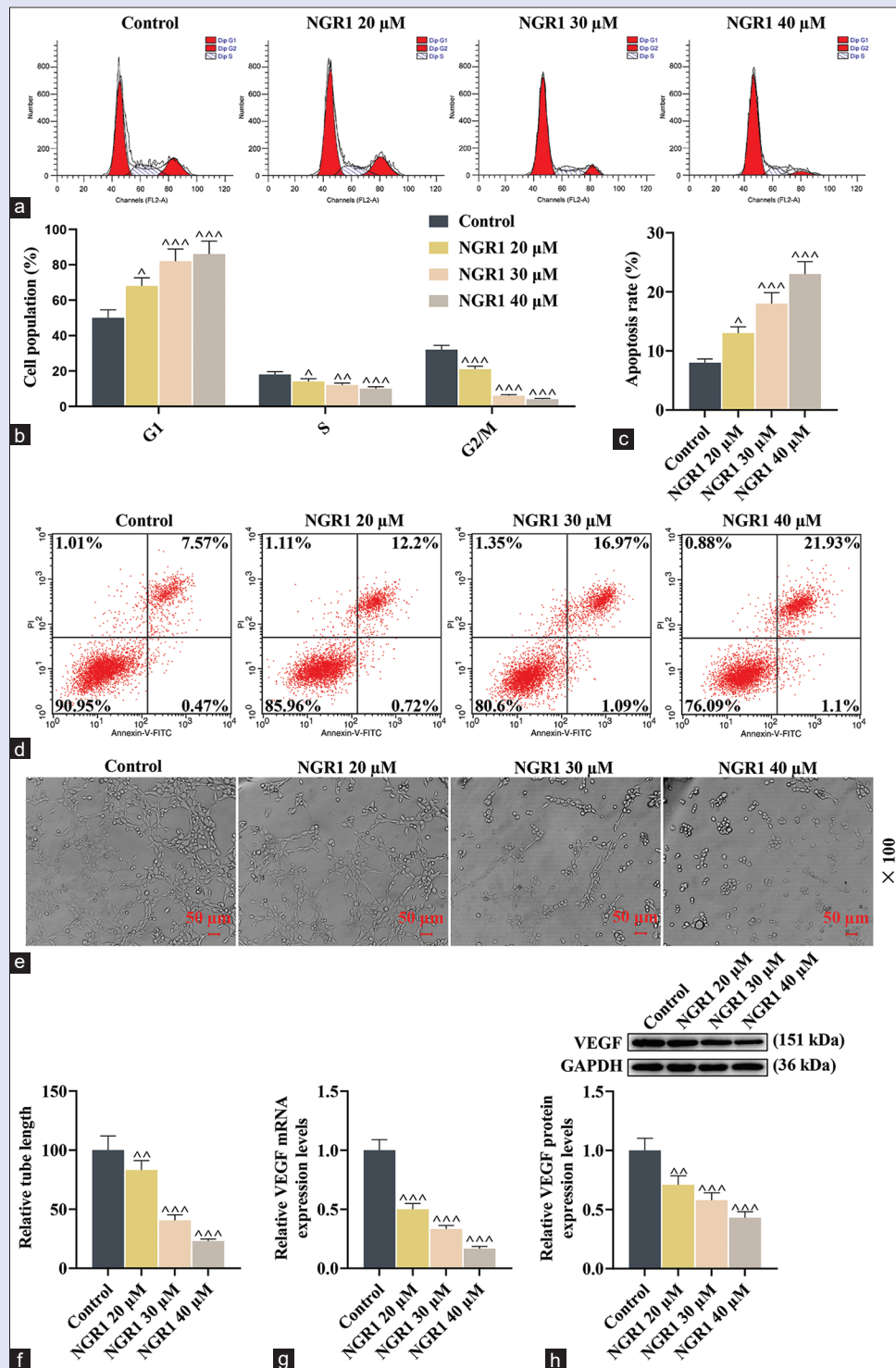


Figure 2: The effect of NGR1 treatment on KEL FIB cells. KEL FIB cells were selected for this experiment and divided into four groups: control group (untreated cells), low NGR1 group (treated with 20 μ M NGR1), medium NGR1 group (treated with 30 μ M NGR1), and high NGR1 group (treated with 40 μ M NGR1). (a and b) Cell cycle was tested by flow cytometry. (a) Representative images of cell cycle at different concentrations. (b) The percentage of cell population in G1, S, and G2/M phases. ^{*}*P* < 0.05, ^{^^}*P* < 0.01, ^{^^^}*P* < 0.001 versus control group. (c, d) NGR1 induced apoptosis of KEL FIB cells. (c) Histogram of apoptosis rate. ^{*}*P* < 0.05, ^{^^}*P* < 0.001 versus control group. (d) Cells with Annexin V-FITC/PI staining were measured by flow cytometry. (e and f) The formation of endothelial tubes was suppressed after NGR1 preconditioning. Tubes' images were observed using an inverted microscope and relative tube length was quantified. Scale bar = 50 μ m ($\times 100$). ^{*}*P* < 0.01, ^{^^}*P* < 0.001 versus control group. (g) NGR1 inhibited the expression of VEGF mRNA in KEL FIB cells. GAPDH was used as the internal control. ^{^^}*P* < 0.001 versus control group. (h) Western blot for VEGF protein. GAPDH was used as the control. The grayscale image and the corresponding relative quantitative figure are provided. ^{*}*P* < 0.01, ^{^^}*P* < 0.001 versus control group. Data are expressed as means \pm SD, and experiments were performed in triplicate. NGR1 = notoginsenoside R1, PI = propidium iodide, SD = standard deviation, VEGF = vascular endothelial growth factor

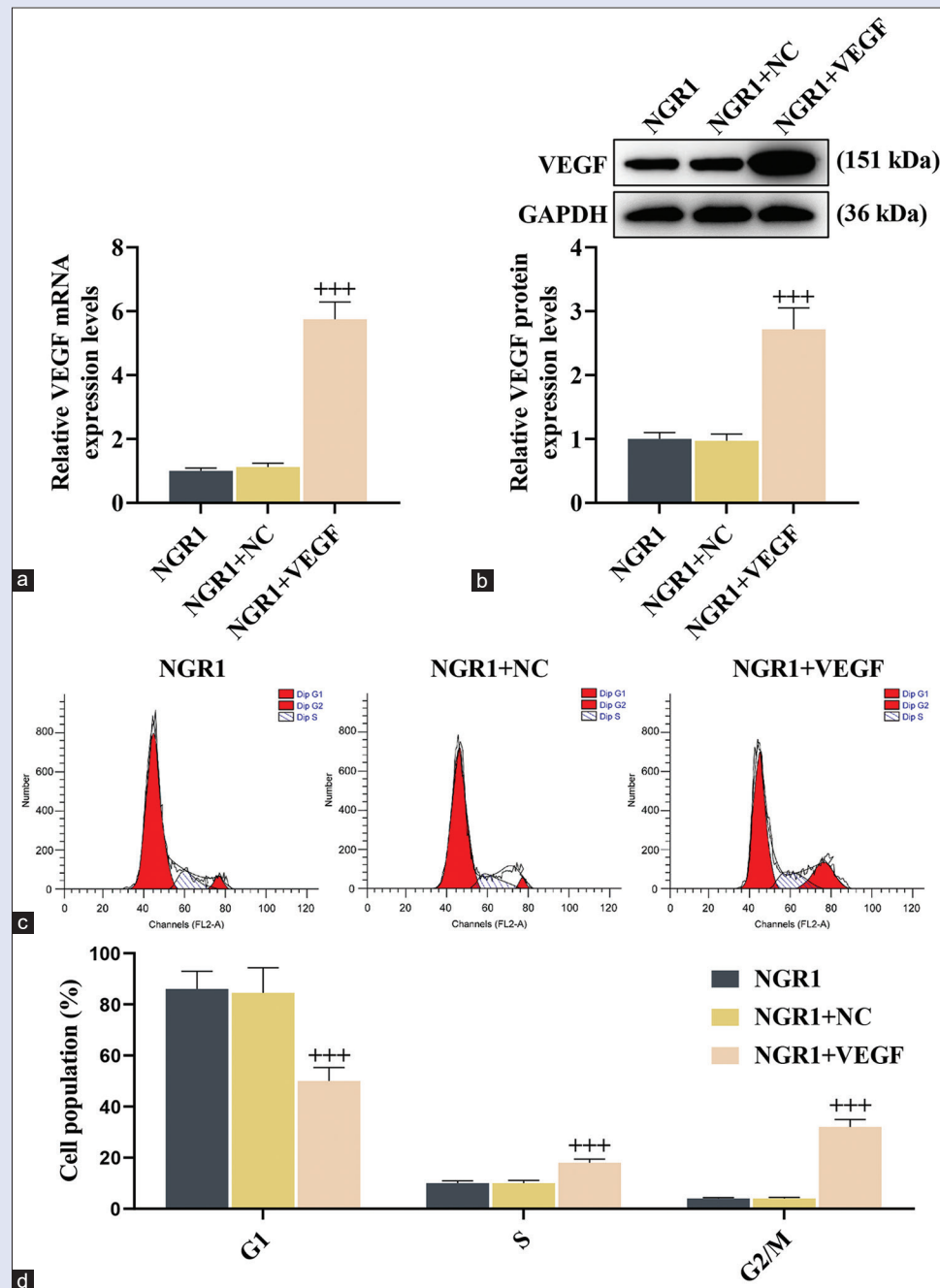


Figure 3: VEGF overexpression exerted a reversal effect on KEL FIB cells pretreated with NGR1. NGR1 concentration of 40 μ M was the most appropriate for the next experiment. Cells were divided into three groups: NGR1 (cells treated with 40 μ M NGR1), NGR1 + NC (cells treated with 40 μ M NGR1 and transfected with pcDNA3.1 negative plasmid), NGR1 + VEGF (cells treated with 40 μ M NGR1 and transfected with pcDNA3-VEGF positive plasmid). (a, b) VEGF overexpression plasmid increased the levels of VEGF in KEL FIB cells. VEGF mRNA expression was detected by quantitative real-time PCR (a). $^{+++}P < 0.001$ versus NGR1 + NC. The protein levels measured by western blot and data quantified by ImageJ are shown (b). $^{+++}P < 0.001$ versus NGR1 + NC. (c and d) VEGF overexpression promoted cell cycle. The typical cell cycle image in the three groups given above (c). The proportions of KEL FIB cells at different stages of cell cycle (d). $^{+++}P < 0.001$ versus NGR1 + NC. Data are expressed as means \pm SD, and experiments were performed in triplicate. NC = negative control, NGR1 = notoginsenoside R1, PCR = polymerase chain reaction, SD = standard deviation, VEGF = vascular endothelial growth factor

indicated that VEGF could be a factor that promoted angiogenesis in the process of keloid formation. Previous studies have also proved that VEGF markedly restrained apoptosis in mesenchymal stem cells (MSC).^[46] In this study, NGR1 inhibits KFB proliferation and may further alleviate keloid injury via downregulating VEGF and subsequent cell growth inhibition.

To sum up, the exploration of NGR1 not only provides a candidate treatment drug for keloid, which may deserve trying out in the future for keloid patients, but also identifies a potential molecular target for keloid therapy with NGR1. However, all the above experiments were carried out at a cellular level (*in vitro*), which proved to be a big challenge to simulate the internal environment completely. Therefore, it is necessary

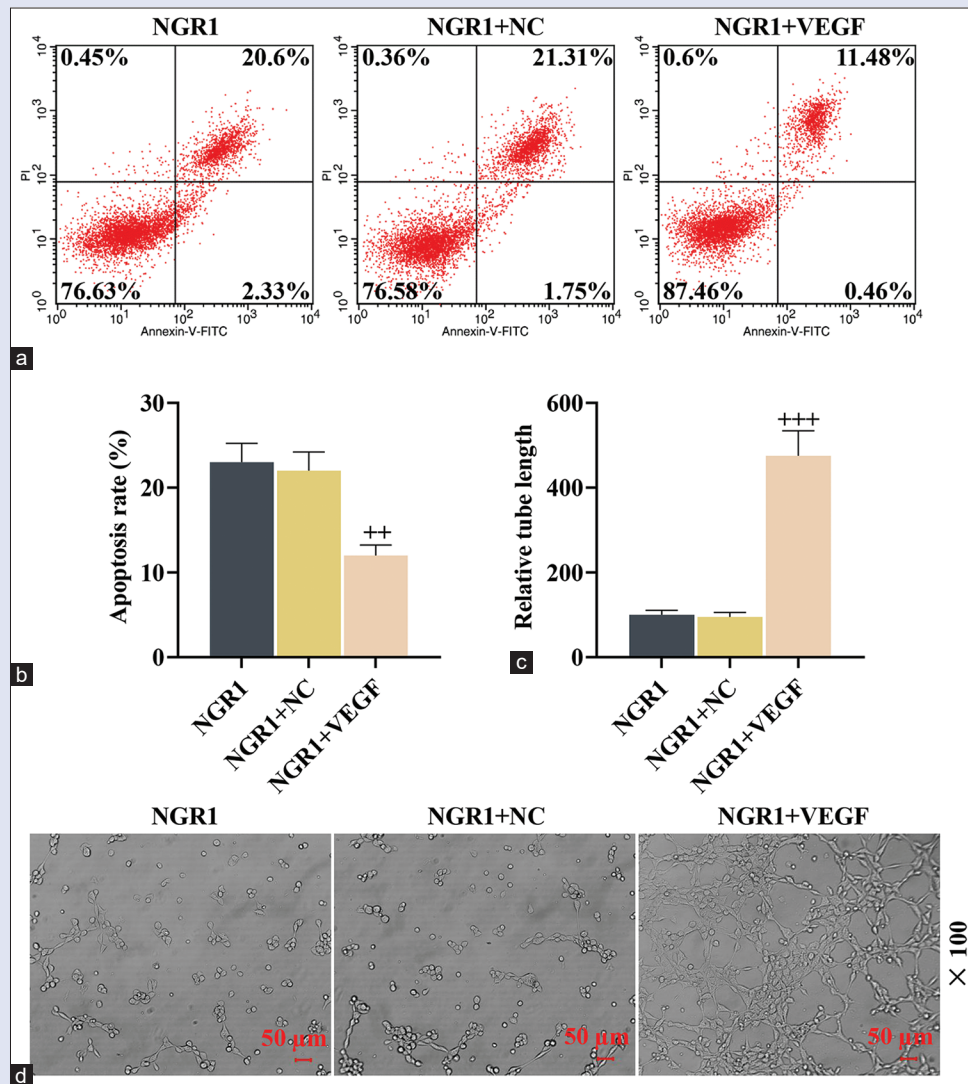


Figure 4: VEGF overexpression suppressed cell apoptosis and promoted tube formation in KEL FIB cells pretreated with Notoginsenoside R1 (NGR1). The cell grouping was consistent with Figure 3. (a and b) VEGF overexpression inhibited the apoptosis of cells treated with NGR1. Apoptosis rate in different groups was detected by flow cytometry. The typical flow cytometry (a) and histogram (b) are shown. $^{**}P < 0.01$ versus NGR1 + NC. (c and d) Tube formation assay was conducted to determine angiogenic responses. Relative tube length was measured with ImageJ software (c). $^{+++}P < 0.001$ versus NGR1 + NC. VEGF overexpression plasmid promoted tube formation compared with NGR1 + NC group (d). Scale bar = 50 μm (×100). Data are expressed as means ± SD, and experiments were performed in triplicate. NC = negative control, NGR1 = notoginsenoside R1, SD = standard deviation, VEGF = vascular endothelial growth factor

to perform *in vivo* studies to confirm the protective effects of NGR1 on keloid injury.

Financial support and sponsorship

Nil.

Conflicts of interest

There are no conflicts of interest.

REFERENCES

- Glass DA 2nd. Current understanding of the genetic causes of keloid formation. *J Investig Dermatol Symp Proc* 2017;18:S50-3.
- Limandjaja GC, Niessen FB, Scheper RJ, Gibbs S. The keloid disorder: Heterogeneity, histopathology, mechanisms and models. *Front Cell Dev Biol* 2020;8:360. doi: 10.3389/fcell.2020.00360.
- Berman B, Maderal A, Raphael B. Keloids and hypertrophic scars: Pathophysiology, classification, and treatment. *Dermatol Surg* 2017;43(Suppl 1):S3-18.
- Ogawa R. Keloid and hypertrophic scars are the result of chronic inflammation in the reticular dermis. *Int J Mol Sci* 2017;18. doi: 10.3390/ijms18030606.
- Zoumalan CI. Topical agents for scar management: Are they effective? *J Drugs Dermatol* 2018;17:421-5.
- Hoang D, Reznik R, Orgel M, Li Q, Mirhadi A, Kulber DA. Surgical excision and adjuvant brachytherapy vs external beam radiation for the effective treatment of keloids: 10-year institutional retrospective analysis. *Aesthet Surg J* 2017;37:212-25.
- He S, Yang Y, Liu X, Huang W, Zhang X, Yang S, *et al.* Compound *Astragalus* and *Salvia miltiorrhiza* extract inhibits cell proliferation, invasion and collagen synthesis in keloid fibroblasts by mediating transforming growth factor-β/Smad pathway. *Br J Dermatol* 2012;166:564-74.
- Chen G, Liang Y, Liang X, Li Q, Liu D. Tanshinone IIA inhibits proliferation and induces apoptosis through the downregulation of survivin in keloid fibroblasts. *Ann Plast Surg* 2016;76:180-6.

9. Xie Y, Fan C, Dong Y, Lynam E, Leavesley DJ, Li K, *et al.* Functional and mechanistic investigation of Shikonin in scarring. *Chem Biol Interact* 2015;228:18-27.
10. Jia C, Xiong M, Wang P, Cui J, Du X, Yang Q, *et al.* Notoginsenoside R1 attenuates atherosclerotic lesions in ApoE deficient mouse model. *PLoS One* 2014;9:e99849.
11. Luo C, Sun Z, Li Z, Zheng L, Zhu X. Notoginsenoside R1 (NGR1) attenuates chronic atrophic gastritis in rats. *Med Sci Monit* 2019;25:1177-86.
12. Zou S, Zhang M, Feng L, Zhou Y, Li L, Ban L. Protective effects of notoginsenoside R1 on cerebral ischemia-reperfusion injury in rats. *Exp Ther Med* 2017;14:6012-6.
13. Su P, Du S, Li H, Li Z, Xin W, Zhang W. Notoginsenoside R1 inhibits oxidized low-density lipoprotein induced inflammatory cytokines production in human endothelial EA.hy926 cells. *Eur J Pharmacol* 2016;770:9-15.
14. Yu Y, Sun G, Luo Y, Wang M, Chen R, Zhang J, *et al.* Cardioprotective effects of Notoginsenoside R1 against ischemia/reperfusion injuries by regulating oxidative stress- and endoplasmic reticulum stress-related signaling pathways. *Sci Rep* 2016;6:21730. doi: 10.1038/srep21730.
15. Fang H, Yang S, Luo Y, Zhang C, Rao Y, Liu R, *et al.* Notoginsenoside R1 inhibits vascular smooth muscle cell proliferation, migration and neointimal hyperplasia through PI3K/Akt signaling. *Sci Rep* 2018;8:7595.
16. Zhu L, Gong X, Gong J, Xuan Y, Fu T, Ni S, *et al.* Notoginsenoside R1 upregulates miR-221-3p expression to alleviate ox-LDL-induced apoptosis, inflammation, and oxidative stress by inhibiting the TLR4/NF- κ B pathway in HUVECs. *Braz J Med Biol Res* 2020;53:e9346. doi: 10.1590/1414-431x20209346.
17. Guo S, Xi X, Li J. Notoginsenoside R1: A systematic review of its pharmacological properties. *Pharmazie*. 2019;74:641-7. doi: 10.1691/ph.2019.9534.
18. Fan C, Chen Q, Ren J, Yang X, Ru J, Zhang H, *et al.* Notoginsenoside R1 suppresses inflammatory signaling and rescues renal ischemia-reperfusion injury in experimental rats. *Med Sci Monit* 2020;26:e920442. doi: 10.12659/MSM.920442
19. Xiao J, Zhu T, Yin YZ, Sun B. Notoginsenoside R1, a unique constituent of *Panax notoginseng*, blinds proinflammatory monocytes to protect against cardiac hypertrophy in ApoE(-/-) mice. *Eur J Pharmacol* 2018;833:441-50.
20. Lei R, Li J, Liu F, Li W, Zhang S, Wang Y, *et al.* HIF-1 α promotes the keloid development through the activation of TGF β /Smad and TLR4/MyD88/NF κ B pathways. *Cell Cycle* 2019;18:3239-50.
21. Wu WS, Wang FS, Yang KD, Huang CC, Kuo YR. Dexamethasone induction of keloid regression through effective suppression of VEGF expression and keloid fibroblast proliferation. *J Invest Dermatol* 2006;126:1264-71.
22. Zhu Y, Wang Y, Jia Y, Xu J, Chai Y. Roxadustat promotes angiogenesis through HIF-1 α /VEGF/VEGFR2 signaling and accelerates cutaneous wound healing in diabetic rats. *Wound Repair Regen* 2019;27:324-34.
23. Wilgus TA. Vascular endothelial growth factor and cutaneous scarring. *Adv Wound Care* 2019;8:671-8.
24. Wise LM, Stuart GS, Real NC, Fleming SB, Mercer AA. VEGF Receptor-2 activation mediated by VEGF-E limits scar tissue formation following cutaneous injury. *Adv Wound Care* 2018;7:283-97.
25. Zhou P, Xie W, Meng X, Zhai Y, Dong X, Zhang X, *et al.* Notoginsenoside R1 ameliorates diabetic retinopathy through PINK1-dependent activation of mitophagy. *Cells* 2019;8:213. doi: 10.3390/cells8030213.
26. Cong S, Xiang L, Yuan X, Bai D, Zhang X. Notoginsenoside R1 up-regulates microRNA-132 to protect human lung fibroblast MRC-5 cells from lipopolysaccharide-caused injury. *Int Immunopharmacol* 2019;68:137-44.
27. Hu Y, Rao SS, Wang ZX, Cao J, Tan YJ, Luo J, *et al.* Exosomes from human umbilical cord blood accelerate cutaneous wound healing through miR-21-3p-mediated promotion of angiogenesis and fibroblast function. *Theranostics* 2018;8:169-84.
28. Livak KJ, Schmittgen TD. Analysis of relative gene expression data using real-time quantitative PCR and the 2(-Delta Delta C (T)) method. *Methods* 2001;25:402-8.
29. Ding JC, Tang ZM, Zhai XX, Chen XH, Li JG, Zhang CX. The effects of Wubeizi ointment on the proliferation of keloid-derived fibroblasts. *Cell Biochem Biophys* 2015;71:431-5.
30. Tang Z, Cao Y, Ding J, Zhai X, Jing M, Wang M, *et al.* Wubeizi ointment suppresses keloid formation through modulation of the mTOR pathway. *BioMed Res Int* 2020;2020:3608372. doi: 10.1155/2020/3608372.
31. Si L, Zhang M, Guan E, Han Q, Liu Y, Long X, *et al.* Resveratrol inhibits proliferation and promotes apoptosis of keloid fibroblasts by targeting HIF-1 α . *J Plast Surg Hand Surg* 2020;54:290-6.
32. Kawarazaki A, Horinaka M, Yasuda S, Numajiri T, Nishino K, Sakai T. Sulforaphane suppresses cell growth and collagen expression of keloid fibroblasts. *Wound Repair Regen* 2017;25:224-33.
33. Li Y, Wang H, Wang R, Lu X, Wang Y, Duan M, *et al.* Pharmacokinetics, tissue distribution and excretion of saponins after intravenous administration of ShenMai injection in rats. *J Chromatogr B Analyt Technol Biomed Life Sci* 2019;1128:121777. doi: 10.1016/j.jchromb.2019.121777.
34. Chen YY, Li Q, Pan CS, Yan L, Fan JY, He K, *et al.* QiShenYiQi Pills, a compound in Chinese medicine, protects against pressure overload-induced cardiac hypertrophy through a multi-component and multi-target mode. *Sci Rep* 2015;5:11802. doi: 10.1038/srep11802.
35. Liu H, Yang J, Yang W, Hu S, Wu Y, Zhao B, *et al.* Focus on notoginsenoside R1 in metabolism and prevention against human diseases. *Drug Des Dev Ther* 2020;14:551-65.
36. Qin HL, Wang XJ, Yang BX, Du B, Yun XL. Notoginsenoside R1 attenuates breast cancer progression by targeting CCND2 and YBX3. *Chin Med J* 2021;134:546-54.
37. Gentile MT, Pastorino O, Bifulco M, Colucci-D'Amato L. HUVEC tube-formation assay to evaluate the impact of natural products on angiogenesis. *J Vis Exp* 2019:e58591. doi: 10.3791/58591.
38. Zhong J, Lu W, Zhang J, Huang M, Lyu W, Ye G, *et al.* Notoginsenoside R1 activates the Ang2/Tie2 pathway to promote angiogenesis. *Phytomedicine* 2020;78:153302. doi: 10.1016/j.phymed.2020.153302.
39. Xu X, Lai Y, Hua ZC. Apoptosis and apoptotic body: disease message and therapeutic target potentials. *Biosci Rep* 2019;39. doi: 10.1042/BSR20180992.
40. Zhang X, Liu W, Wei S. Luteolin affects keloid fibroblast proliferation and apoptosis by regulating FRAT1 gene expression. *Cell Mol Biol* 2020;66:185-90.
41. Gao SW, Liu F. Novel insights into cell cycle regulation of cell fate determination. *J Zhejiang Univ Sci B* 2019;20:467-75.
42. Ji J, Tian Y, Zhu YQ, Zhang LY, Ji SJ, Huan J, *et al.* Ionizing irradiation inhibits keloid fibroblast cell proliferation and induces premature cellular senescence. *J Dermatol* 2015;42:56-63.
43. Zhang T, Wang XF, Wang ZC, Lou D, Fang QQ, Hu YY, *et al.* Current potential therapeutic strategies targeting the TGF β /Smad signaling pathway to attenuate keloid and hypertrophic scar formation. *Biomed Pharmacother* 2020;129:110287. doi: 10.1016/j.biopha.2020.110287.
44. Abdu Allah AMK, Mohammed KI, Farag AGA, Hagag MM, Essam M, Tayel NR. Interleukin-6 serum level and gene polymorphism in keloid patients. *Cell Mol Biol (Noisy-le-Grand, France)* 2019;65:43-8.
45. Lee YS, Liang YC, Wu P, Kulber DA, Tanabe K, Chuong CM, *et al.* STAT3 signalling pathway is implicated in keloid pathogenesis by preliminary transcriptome and open chromatin analyses. *Exp Dermatol* 2019;28:480-4.
46. Deng S, Xiang JJ, Shen YY, Lin SY, Zeng YQ, Shen JP. [Effects of VEGF-Notch Signaling Pathway on Proliferation and Apoptosis of Bone Marrow MSC in Patients with Aplastic Anemia]. *Zhongguo Shi Yan Xue Ye Xue Za Zhi* 2019;27:1925-32.